1388 *Biochemistry* **2010,** *49,* 1388–1395
DOI: 10.1021/bi9018225

BIOCHEMISTRY
including biophysical chemistry & molecular biology
Article

Roles for Cationic Residues at the Quinolinic Acid Binding Site of Quinolinate Phosphoribosyltransferase[†]

Zainab Bello[‡] and Charles Grubmeyer*

Fels Institute for Cancer Research and Molecular Biology and Department of Biochemistry, Temple University School of Medicine, 3307 North Broad Street, Philadelphia, Pennsylvania 19140 [‡]Present address: Department of Biological Chemistry, University of Michigan Medical School, Ann Arbor, MI 48109-5606.

Received October 25, 2009; Revised Manuscript Received December 28, 2009

ABSTRACT: Quinolinic acid phosphoribosyltransferase (QAPRTase, EC 2.4.2.19) forms nicotinate mononucleotide (NAMN) from quinolinic acid (QA) and 5-phosphoribosyl 1-pyrophosphate (PRPP). Previously determined crystal structures of QAPRTase·QA and QAPRTase·PA·PRPP complexes show positively charged residues (Arg118, Arg152, Arg175, Lys185, and His188) lining the QA binding site. To assess the roles of these residues in the *Salmonella typhimurium* QAPRTase reaction, they were individually mutated to alanine and the recombinant proteins overexpressed and purified from a recombineered *Escherichia coli* strain that lacks the QAPRTase gene. Gel filtration indicated that the mutations did not affect the dimeric aggregation state of the enzymes. Arg175 is critical for the QAPRTase reaction, and its mutation to alanine produced an inactive enzyme. The k_{cat} values for R152A and K185A were reduced by 33-fold and 625-fold, and binding affinity of PRPP and QA to the enzymes decreased. R152A and K185A mutants displayed 116-fold and 83-fold increases in activity toward the normally inactive QA analogue, nicotinic acid (NA), indicating roles for these residues in defining the substrate specificity of QAPRTase. Moreover, K185A QAPRTase displayed a 300-fold higher k_{cat}/K_m for NA over the natural substrate QA. Pre-steady-state analysis of K185A with QA revealed a burst of nucleotide formation followed by a slower steady-state rate, unlike the linear kinetics of WT. Intriguingly, pre-steady-state analysis of K185A with NA produced a rapid but linear rate for NAMN formation. The result implies a critical role for Lys185 in the chemistry of the QAPRTase intermediate. Arg118 is an essential residue that reaches across the dimer interface. Mutation of Arg118 to alanine resulted in 5000-fold decrease in k_{cat} value and a decrease in the binding affinity of QA and PRPP to R152A. Equimolar mixtures of R118A with inactive or virtually inactive mutants produced approximately 50% of the enzymatic activity of WT, establishing an interfacial role for Arg118 during catalysis.

Quinolinate phosphoribosyltransferase (QAPRTase,[1] EC 2.4.2.19) is a type II phosphoribosyltransferase (PRTase) that participates in the *de novo* biosynthesis of the pyridine coenzyme, NAD (*1*, *2*). Recently, nicotinate phosphoribosyltransferase (NAPRTase) and nicotinamide phosphoribosyltransferase (NMPRTase), involved in the salvage pathways of NAD biosynthesis, have been classified as type II PRTases (*3*−*5*). The type II PRTases catalyze the transfer of a phosphoribosyl moiety from 5-phosphoribosyl 1-pyrophosphate (PRPP) to their specific substrates. The phosphoribosyl transfer reaction catalyzed by QAPRTase is linked to an irreversible decarboxylation reaction at position 2 of the quinolinic acid (QA) ring, with no cofactor requirement (*2*, *6*).

The *nadC* gene of *Salmonella typhimurium* which encodes QAPRTase is one of the three nonessential genes involved in *de novo* NAD biosynthesis (*7*). Unlike the other two genes (*nadA* (L-aspartate oxidase) and *nadB* (quinolinate synthase)), which are known to be regulated by the *NadI* repressor, the *nadC* gene is not genetically controlled (*8*). However, QAPRTase is specific for QA and cannot use its analogue nicotinic acid (NA). QA differs from NA by the presence of the negatively charged carboxylate group at position 2 of the molecule (Figure 1). In the salvage pathway of NAD biosynthesis, NAPRTase converts NA to NAMN. Like QAPRTase, NAPRTase shows a high degree of specificity for its substrate, as indicated in genetic and enzymological studies (*9*, *10*). Appropriate bacterial strains carrying *nadC* (to block QAPRTase activity) or *pncB* mutations (to block NAPRTase) show auxotrophies that are not relieved by NA and QA, respectively (*9*). Additionally, NA does not detectably inhibit QAPRTase, whereas several pyridine analogues with negative charges at the 2 position have been shown to be effective inhibitors of the enzyme (*11*, *12*). Although crystal structures are available for all of the type II PRTases, it remains unknown how the enzymes discriminate among their respective substrates.

The reaction catalyzed by QAPRTase follows an ordered-sequential mechanism, in which QA binds first, followed by PRPP, releasing NAMN and then PP_i (*13*). The phosphoribosyl transfer reaction that forms the putative quinolinate mononucleotide (QAMN) intermediate is thought to precede the decarboxylation of the QAMN to form NAMN ((*14*); a recent theoretical study (*15*) has reviewed this idea). QAMN has never been isolated or synthesized, and its chemical stability and properties are unknown. Thus, it is not clear if the decarboxylation is enzymatic

[†]Supported by NIH Grant GM48623 to C.G.
*To whom correspondence should be addressed. Phone: (215) 707-4495. Fax: (215) 707-5529. E-mail: ctg@temple.edu.
[1]Abbreviations: QA, quinolinic acid; PA, phthalic acid; PRPP, 5-phosphoribosyl 1-pyrophosphate; NAMN, nicotinate mononucleotide; PP_i, pyrophosphate; NAPRTase, nicotinate phosphoribosyltransferase; QAMN, quinolinate mononucleotide; PRPCP, 5-phosphoribosyl 1-(β-methylene)pyrophosphate.

 Published on Web 01/04/2010

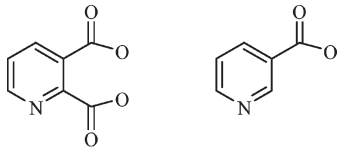

FIGURE 1: Chemical structures of quinolinate and nicotinate.

or spontaneous. Based on inhibition studies, the putative QAMN intermediate was proposed to decarboxylate via an ylide mechanism (*12*, *16*, *17*). The ylide mechanism has also been proposed for the decarboxylation of orotidine 5′-monophosphate by OMP decarboxylase, which, like QAPRTase, is an α/β barrel enzyme and has no cofactor requirement (*18*). Among cofactorless decarboxylases, a lysine amino group was recently proposed to act as the initial carboxyl receptor in a bacterial oxaloacetate decarboxylase (*19*). Studies with model compounds showed that nonenzymatic decarboxylation of pyridine-2-carboxylic acids substituted with a carboxyl group at position 3 occurred spontaneously (*16*, *17*). However, the rate of the QAPRTase reaction is 5 orders of magnitude faster than the spontaneous decarboxylation of the model compounds. QAPRTase may thus be involved in the decarboxylation step. Positively charged residues in the actives site of the enzyme might directly stabilize the negative charge at the 2 position of QA after decarboxylation of the putative QAMN intermediate (*2*, *6*).

Crystal structures of substrate-bound complexes of QAPRTase from various organisms provide insights into the structure–function relationship of the enzyme (*2*, *6*, *20*–*22*). The active site of the enzyme is located at the C-terminal α/β barrel domain of one subunit, which is bordered by the N-terminal domain of the adjacent subunit, forming a head-to-tail, domain-swapped dimer (*2*). In the crystal structure of *S. typhimurium* QAPRTase, the QA binding site (Figure 2) is composed of the following positively charged residues: Arg118′ (sequence numbering is based on the mature *Salmonella* enzyme; the prime designates a residue from the adjacent subunit), Arg152, Arg175, Lys185, and His188. One of the oxygen atoms of the 2-carboxylate of PA (Figure 2) forms hydrogen bonds with the amino nitrogen of Lys185 (2.8 Å), and it is 3 Å away from NH1 of Arg118′. Arg118′ is involved in an extensive hydrogen bonding. The *Mycobacterium tuberculosis* QAPRTase·PA·PRPPC ternary analogue complex shown here demonstrated that, in addition to interacting with QA, NH1 of Arg118′ is within hydrogen-bonding distance of the α-phosphate of PRPP (*6*). The second oxygen atom of the 2-carboxylate of PA is 3.3 Å away from the Nε of Arg118′ and forms a hydrogen bond with the main chain N of Arg152. These residues may be important for binding of QA or exclusion of NA. Additionally, the negative charge at the 2 position of the QA ring after decarboxylation of the QAMN intermediate might be stabilized indirectly, by inductive electron withdrawal through interactions of Arg152 and Arg175 (*2*, *6*). Arg175 makes a bidentate hydrogen bond with the oxygen atoms of the C3 carboxylate of PA, while the Nε of Arg152 is seen to interact with one of the oxygen atoms of PA. His188 (not shown) is also in the wall of the active site, but its closest approach to QA (via the C2 carboxylate) is 8.3 Å.

The origin of the striking base specificity of QAPRTase remains a major issue. It is easiest to imagine that NA simply fails to form the panoply of hydrogen bonds that QA can. In line with this, NA is a particularly poor inhibitor of QAPRTase (*11*).

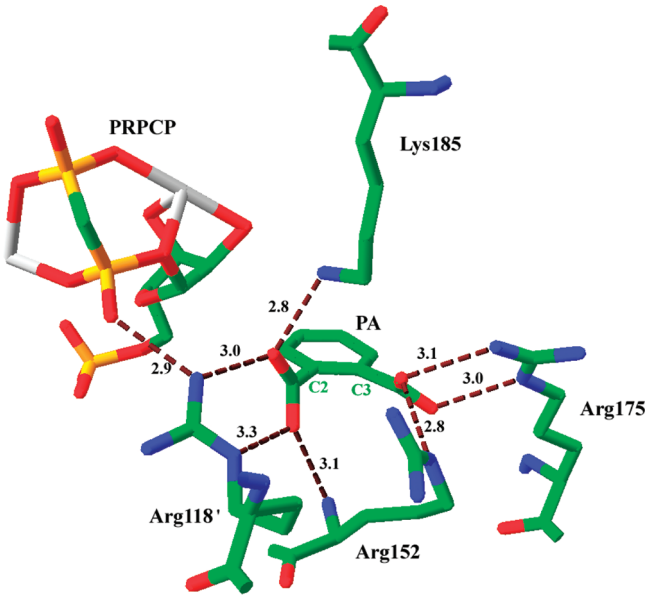

FIGURE 2: Binding site for QA in the *M. tuberculosis* QAPRTase·PA·PRPCP·Mn^{2+} Michaelis complex (PDB entry 1QPR). Residues that interact with QA are shown, and their hydrogen-bonding distances are represented in Å. The prime on Arg118′ designates a residue from the adjacent subunit. C2 and C3 are designations of the homologous positions on QA. The two Mn^{2+} coordinated by PRPC are shown in gray. This figure was generated using SwissPDB Viewer (*23*).

That poor binding may extend to poor catalysis; in particular, a dual interaction of Arg118′ with both the 2-carboxylate of QA and the pyrophosphate portion of PRPP may allow QA to orient for catalysis, whereas NA may not. Alternatives would include the proposal that NA may be able to undergo weak and nonproductive "wrong way" binding in which the C3 carboxylate occupies the site normally bound by the 2-carboxylate of QA, with the N1 of NA now occupying the site normally occupied by the C4 of QA. In thymidylate synthase, exclusion of dCMP from the dUMP site appeared to arise by steric exclusion mediated by Asn229, but study of indiscriminant D229N mutants suggests a more complex mechanism including rearrangement of active site residues. The potential mobility of Lys185, and its somewhat "kinked" side chain conformation, makes a role for exclusion of NA a possibility. However, examination of structures does not seem to support an alternative position of the Lys185 side chain that blocks access to the QA site by NA.

The positively charged residues that line the QA binding site are thus base binding residues, candidates for base specificity, and might act directly or indirectly to stabilize the QAMN intermediate. In a recent characterization of the human QAPRTase the homologous residues were identified, and preliminary characterization of mutants was reported (*21*). In this paper, the residues were mutated individually to alanine, in order to explore their contribution to catalysis. The kinetic characterization of the mutant enzymes with respect to WT is presented, allowing conclusions about the origin of the base specificity of the enzyme.

MATERIALS AND METHODS

Materials. Materials used have been previously described (*24*). SDS–PAGE (14–20%) gels were from Lonza Biosciences. [^{14}C]NA was obtained from Sigma.

Overexpression and Purification of Enzymes. Construction of ZB100, the deleted *nadC* strain of BL21(DE3), has been

described (*24*). The QuikChange site-directed mutagenesis kit (Stratagene) was used to carry out the mutations. The following primers were used to construct the mutants: R118A (forward, G CTG ACC GGC GAG **GCG** ACG GCG CTA AAC TTT GTC; reverse, GAC AAA GTT TAG CGC CGT **CGC** CTC GCC GGT CAG C); R152A (forward, C CAG TTG CTC GAC ACG **GCG** AAA ACG CTG CCG GGT C; reverse, G ACC CGG CAG CGT TTT **CGC** CGT GTC GAG CAA CTG G); K153A (forward, CAG TTG CTC GAC ACG CGT **GCG** ACG CTG CCG GGT CTG CGC; reverse, GCG CAG ACC CGG CAG CGT **CGC** ACG CGT GTC GAG CAA CTG); R175A (forward, C GGC GGC GCC AAT CAT **GCG** CTG GGC CTC ACT GAC G; reverse, C GTC AGT GAG GCC CAG **CGC** ATG ATT GGC GCC GCC G); K185A (forward, CTC ACT GAC GCG TTC CTG ATT **GCG** GAA AAC CAT ATT ATC GCC TCC; reverse, GGA GGC GAT AAT ATG GTT TTC **CGC** AAT CAG GAA CGC GTC AGT GAG); H188A (forward, C GCG TTC CTG ATT AAA GAA AAC **GCG** ATT ATC GCC TCC GGT TCG GTT C; reverse, G AAC CGA ACC GGA GGC GAT AAT **CGC** GTT TTC TTT AAT CAG GAA CGC G), with the mutated codon in bold. The ZB100 strain used for protein expression was transformed with the mutant plasmids following standard procedure. The mutant enzymes were overexpressed and purified as previously described (*24*).

Characterization of Mutant QAPRTases. The aggregation state, equilibrium binding of [^{14}C]PRPP and [^{3}H]QA, and QAPRTase activity of WT and mutant enzyme forms were assayed as described (*24*).

Pre-Steady-State Measurements. Pre-steady-state analysis for the formation of [^{3}H]NAMN and [^{14}C]NAMN using [^{3}H]QA and [^{14}C]NA as substrates, respectively, was carried out. Rapid quench experiments were carried out at 25 °C in buffer QA using an RQF-3 chemical-quench-flow apparatus (KinTek Instruments). Reactions were initiated when 15 μL of enzyme (80 μM) preequilibrated with 2 mM [^{3}H]QA or [^{14}C]NA was mixed with 15 μL of PRPP (8 mM) in buffer QA. Reaction times ranged from 1 s to 10 min. Reactions were quenched with 2 M HCl and collected in 1.5 mL Eppendorf tubes. After all of the samples were collected, the tubes were centrifuged at 3000*g* for 2 min to remove the denatured protein. Aliquots of 10 μL of the quenched sample were spotted and chromatographed on 3MM Whatman paper with a 4:6 mixture of 1 M ammonium acetate:95% ethanol. Under the given conditions, QA and NAMN have R_f values of 0.25 and 0.4, respectively. The [^{3}H]QA and [^{3}H]NAMN were quantitated as described previously (*24*). Control experiments in the absence of enzyme in which the reaction was quenched with HCl determined the background activity. Formation of NAMN by R118A and K185A using [^{3}H]QA was performed by manual mixing. The data for the product formed by the reaction of K185A with [^{3}H]QA were fitted to the burst equation (eq 1) (*25*):

$$[Y] = A(1 - e^{-k_1 t}) + k_{ss} \quad (1)$$

where A is the burst amplitude, k_1, the pre-steady-state rate constant for product formation, t, time, and k_{ss}, the steady-state rate of product formation.

Alternative Substrates for Mutant Enzymes. 2,4-Pyridinedicarboxylic acid, 2,5-pyridinedicarboxylic acid, 2,6-pyridinedicarboxylic acid, 3,4-pyridinedicarboxylic acid, 3,5-pyridinedicarboxylic acid, nicotinamide, pyridine-4-carboxylic acid, 6-aminonicotinic acid, and NA were incubated individually with WT and mutant enzymes under standard radiolabel assay conditions (*24*). Reaction products were visualized under 254 nm UV light after chromatographic separation of products from the transfer assay. The reaction mixture contained 500 μg of mutant enzyme, 0.5 mM alternative substrate, and 2 mM PRPP in a 200 μL reaction volume. The reaction mixtures were incubated for 3 h at 30 °C, inactivated with 2 M HCl, and centrifuged for 5 min (14800*g*) in a microcentrifuge. The supernatant (25 μL) was applied to 3MM Whatman paper and developed as described (*24*). The formation of [^{14}C]NAMN by WT and R152A using [^{14}C]NA as a substrate was measured by the radiolabel transfer assay.

Restoration of Activities of Mutant Enzymes by R118A Complementation. Heterodimers of R118A with mutant enzymes (R152A, K153A, R175A, and K185A) were formed individually by mixing equal concentrations (2 mg/mL) of the enzymes in buffer QA containing 1 mM DTT and incubating them for 3 h in ice. The enzymatic activities of the heterodimers were determined by the standard spectrophotometric assay.

RESULTS

The Hydrogen Bond Network in the QA Binding Site. The cationic nature of the quinolinate binding sites of all known QAPRTases has been noted (*2*, *6*, *21*, *22*). Close examination of X-ray structures reveals an intricate web of deduced hydrogen bonding, exemplified by the structure of the *Mycobacterium* ternary substrate analogue complex in Figure 2, which is similar to a recent structure of the yeast enzyme ((*22*); bond lengths are for the complex shown here and vary somewhat with other complexes, analogues, and species). The side chain of Lys185 forms a 2.8 Å hydrogen bond to one C2 carboxylate oxygen, which also interacts (2.95 Å) with NH1 of Arg118′. Arg118 also interacts through its NE with the other C2 carboxylate oxygen (3.3 Å) and, via NH1, with an α-phosphate oxygen of PRPP (2.9 Å). The C2 carboxylate forms a fourth deduced hydrogen bond (3.1 Å) with Arg152 through the main chain N of the latter. At the C3 carboxylate, three apparent hydrogen bonds, from NE of Arg152 (2.8 Å) and from NE (3.0 Å) and NH1 (3.1 Å), are formed. Thus, each of the two carboxylates and each of the Arg residues makes multidentate hydrogen bonds that could serve to read substrate identity. Lys185, which forms a single hydrogen bond, appears more free to move, and a recent structure of the binary complex of QA with the yeast enzyme shows Lys185 interacting via a water molecule with a C3 carboxylate oxygen (*22*).

Examination of a large sequence library (Materials and Methods) showed that the residues lining the QA site were highly conserved (Figure 3). Arg152, Lys153, Arg175, and His188 were all absolutely conserved. Arg118 and Lys185 were conserved, except for replacement by Lys and Phe, respectively, in *Rhodopseudomonas palustris*. The extreme sequence conservation is in keeping with important functional roles.

Expression and Purification of Mutant QAPRTases. The overexpression and purification of the mutant enzymes produced 200−250 mg of protein/6 L of culture and were similar to that of the WT enzyme. The mutant enzymes appeared homogeneous as assessed by SDS−PAGE.

Aggregation State of Mutant QAPRTases. Gel filtration of the mutant enzymes under native conditions was performed on a Superdex 200 column. All mutant enzymes eluted at the same position as WT (data not shown), with similar peak widths at half-height, indicating that the enzymes were stably dimeric with molecular masses of 65 kDa, as predicted for WT (64856 (*26*)).

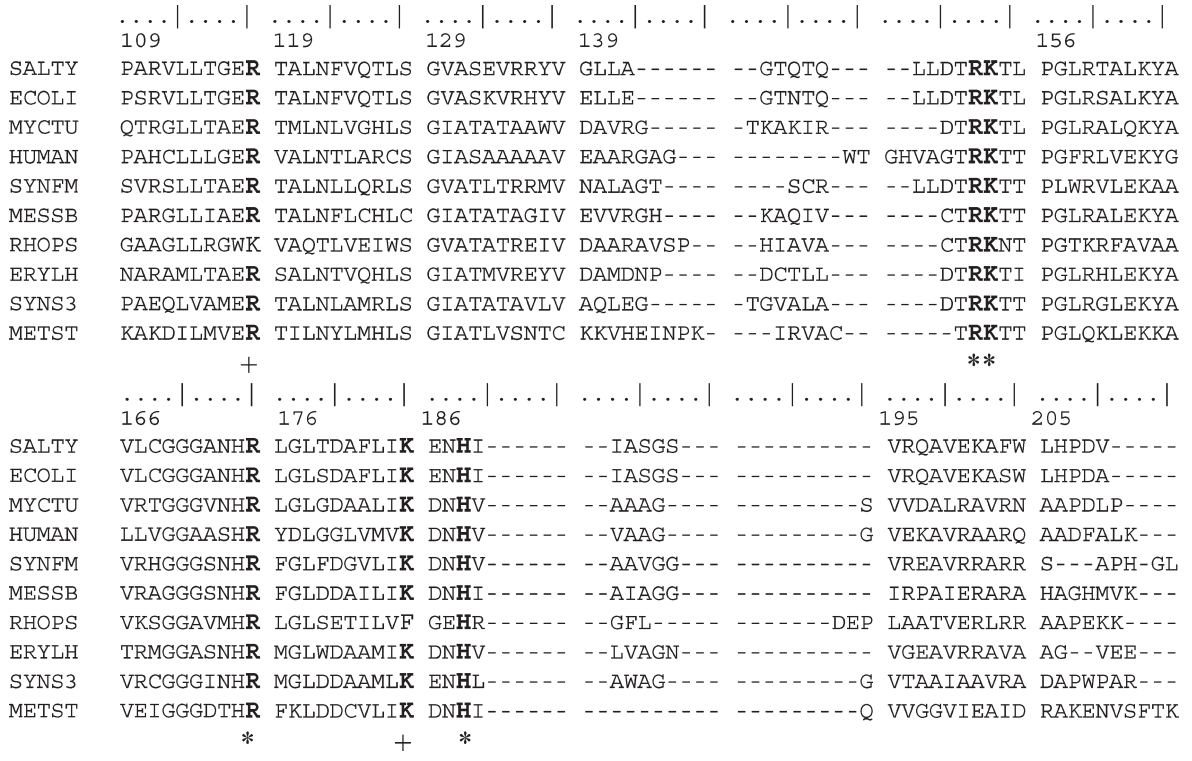

FIGURE 3: Partial sequence alignment of QAPRTase from various organisms. Ten of the 230 sequences aligned as described in Materials and Methods are displayed. Sequences are as follows: SALTY, *S. typhimurium* LT2; ECOLI, *Escherichia coli* K-12; MYCTU, *M. tuberculosis* H37Rv; HUMAN, *Homo sapiens*; SYNFM, *Syntrophobacter fumaroxidans*; MESSB, *Mesorhizobium* sp. BNC1; RHOPS, *R. palustris* BisB5; ERYLH, *Erythrobacter litoralis*; SYNS3, *Synechococcus* sp. CC9311; METST, *Methanosphaera stadtmanae*. Residue numbering at the top is from the mature *S. typhimurium* protein sequence. Conserved residues are indicated in bold, absolutely conserved residues are marked with an *, and highly conserved residues are marked with a + underneath the alignments.

Steady-State Kinetic Measurement for Mutants. Mutation of the residues lining the QA binding site had large impacts on catalytic activity. The steady-state kinetic constants for WT and mutant enzymes are summarized in Table 1. The mutation of Arg118 diminished $k_{cat}/K_{m,PRPP}$ for R118A by 281000-fold compared to WT, indicating the importance of Arg118 in catalysis. This reduction was a result of a 5000-fold lower k_{cat} value and approximately 55-fold elevated $K_{m,PRPP}$ value. The $k_{cat}/K_{m,QA}$ for R118A is reduced by 25000-fold, due to the 5000-fold reduction in k_{cat} and a 5-fold increase in $K_{m,QA}$ value.

Lys185 and Arg152, which interact with the 2-carboxylate and 3-carboxylate of QA, respectively, gave, as expected, decreases in activity for their mutations. Removal of the side chain of Lys185 resulted in a 625-fold decrease in k_{cat}, with a 38-fold higher $K_{m,PRPP}$ and a 55-fold increase in $K_{m,QA}$ causing a 34000-fold decrease in $k_{cat}/K_{m,QA}$ and 25000-fold reduction in $k_{cat}/K_{m,PRPP}$ value. For R152A, k_{cat} decreased by 33-fold, with a 15-fold increase in $K_{m,PRPP}$ and 10-fold increase in $K_{m,QA}$ leading to a 500-fold and 370-fold reduction in $k_{cat}/K_{m,PRPP}$ and $k_{cat}/K_{m,QA}$, respectively.

No measurable activity was detected for R175A, indicating that Arg175 is essential for catalysis. The undetectable activity of R175A like that of K153A (*24*) suggests that activities of other extremely sluggish mutants described here and in the preceding paper (*24*) are intrinsic to those mutant enzymes and not a result of contamination by active enzymes.

Mutation of the absolutely conserved His188 to alanine did not affect the ability of the enzyme to catalyze the QAPR Tase reaction, as the k_{cat} was similar to that of WT. The $K_{m,PRPP}$ value increased by 10-fold, leading to a 10-fold reduction in $k_{cat}/K_{m,PRPP}$ H188A. With the exception of His188, the steady-state results indicate that all of the residues at the QA binding site of QAPRTase are important for catalysis.

Binding of PRPP and QA to the Mutant Enzymes. The effect on formation of binary complexes of mutant QAPRTase was determined by equilibrium binding experiments with [^{3}H]QA and [^{14}C]PRPP by centrifugal dialysis (Table 1). Surprisingly, a reduced binding affinity for PRPP was observed for all of the mutant enzymes, though most of their mutated residues do not directly interact with PRPP as demonstrated from the crystal structures. A 10-fold increase was measured for $K_{D,PRPP}$ for H188A, in agreement with its K_m value. The $K_{D,PRPP}$ for R152A was approximately 1 mM, almost 18-fold higher than WT and in agreement with its $K_{m,PRPP}$ value. The binding of [^{14}C]PRPP to R118A, R175A, and K185A mutant enzymes was not detected by centrifugal dialysis, indicating $K_{D,PRPP}$ values that are greater than 1 mM.

The binding of PRPP to the mutants in the presence of the QA analogue, PA, which tightens binding of PRPP in WT, had no effect on the K_D values of PRPP (data not shown).

The K_D value of QA for R152A was 260 μM, 10-fold higher than that of WT and consistent with its K_m value. For the binding of [^{3}H]QA to R118A, the K_D value measured is represented by Scatchard analysis shown in Figure 4. Consistent with the $K_{m,QA}$, a 5-fold higher K_D value for QA was measured for R118A. Binding of [^{3}H]QA was not detected for R175A and K185A mutant enzymes, indicating K_D values greater than 1 mM.

Alternative Substrates. Alternative substrates were employed to test whether there was a change in base specificity of mutant QAPRTase. To assess the contribution of Arg152 and Lys185 in substrate discrimination, the ability of their respective alanine mutants to carry out the QAPRTase reaction was tested

Table 1: Steady-State Kinetic Parameters for WT and Mutant QAPRTases

kinetic constant	WT	R118A	K185A	R152A	H188A
k_{cat} (s^{-1})	1.0 ± 0.10	2.4×10^{-4}	1.6×10^{-3}	0.03	1.0 ± 0.02
$K_{m,QA}$ (μM)	27 ± 6	136 ± 20	1478 ± 441	278 ± 23	67 ± 5
$k_{cat}/K_{m,QA}$ (μM^{-1} s^{-1})	3.7×10^{-2}	1.5×10^{-6}	1.1×10^{-6}	1.0×10^{-4}	1.6×10^{-2}
$K_{m,PRPP}$ (μM)	57 ± 7	3138 ± 800	2181 ± 500	832 ± 180	547 ± 23
$k_{cat}/K_{m,PRPP}$ (μM^{-1} s^{-1})	1.8×10^{-2}	6.4×10^{-8}	7.3×10^{-7}	3.5×10^{-5}	1.8×10^{-3}
$K_{D,QA}$ (μM)	25 ± 7	128 ± 14	ND[a]	261 ± 38	90 ± 15
n	2.0 ± 0.1	1.9 ± 0.1			1.8 ± 0.3
$K_{D,PRPP}$ (μM)	53 ± 11	ND	ND	~1000	480 ± 75
n					1.7 ± 0.3

[a]ND, not detected.

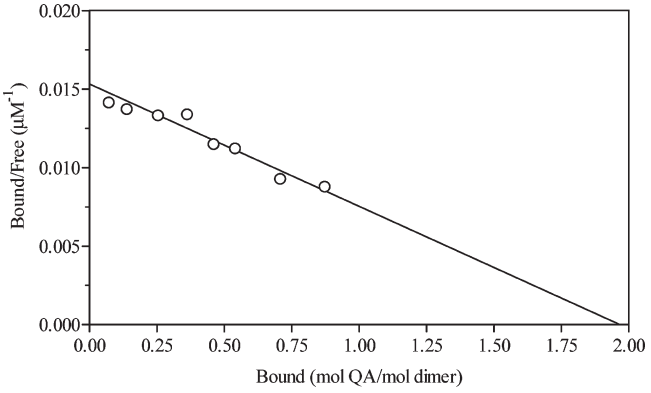

FIGURE 4: Scatchard plot for binding of R118A to [^{3}H]QA. The value of K_D was 128 μM, with an n value of 1.9 mol of [^{3}H]QA/mol of QAPRTase dimer.

using various pyridine analogues. With the exception of NA and 6-aminonicotinic acid, all other QA analogues investigated were not detectably utilized by the mutant enzymes. Formation of NAMN by WT enzyme using NA as a substrate was detected by the radiolabel transfer assay. The specific activity of WT with NA at 1 mM and 2 mM PRPP was 0.0006 unit mg^{-1}. This rate represents a 2000-fold reduction in comparison to its activity of 1.2 units mg^{-1} with 1 mM QA as the substrate. The specificity of R152A for QA and NA is more relaxed than that of WT. A specific activity of 0.07 unit mg^{-1} was measured for the reaction of R152A with NA versus 0.1 unit mg^{-1} using the natural QA substrate. R152A uses NA 116-fold better than WT does. Detailed steady-state kinetic analysis for WT or R152A with NA was not performed.

K185A exhibited an 83-fold higher specific activity for its ability to utilize NA than the WT enzyme did with NA as a substrate. Remarkably, K185A showed a strong preference for NA over QA. Its activity with NA was sufficient to allow measurement of kinetic parameters (Table 2) by the spectrophotometric assay. A 31-fold elevation was observed in $k_{cat,NA}$ compared to the $k_{cat,QA}$ value for the mutant enzyme. The $K_{m,NA}$ value for K185A decreased by 10-fold and $K_{m,PRPP(NA)}$ decreased by 6-fold in comparison to the respective K_m values with the natural QA substrate. The values of $k_{cat}/K_{m,NA}$ and $k_{cat}/K_{m,PRPP(NA)}$ are greater by 300-fold and 178-fold, respectively, in comparison to the values with QA as the substrate. K185A was the only mutant to detectably utilize 6-aminonicotinic acid as a substrate.

Pre-Steady-State Kinetics. It has previously been shown that the chemistry step in the QAPRTase reaction is rate limiting as evidenced from the linear rate in NAMN formation in the pre steady state (*13*, *24*). The pre-steady-state rate of NAMN

Table 2: Comparison of Kinetic Parameters of K185A Using NA as an Alternate Substrate

substrate	k_{cat} (s^{-1})	K_m (μM)	k_{cat}/K_m (μM^{-1} s^{-1})
QA	1.6×10^{-3}	1478 ± 441	1.1×10^{-6}
NA	4.8×10^{-2}	151 ± 13	3.2×10^{-4}

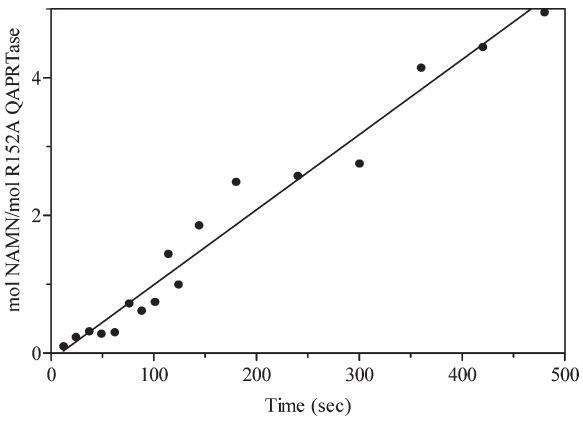

FIGURE 5: Pre-steady-state kinetics of [^{3}H]NAMN formation by R152A with [^{3}H]QA. Rapid mixing was performed in a Kintek chemical-quench-flow apparatus as described in Materials and Methods. The solid line represents a linear least-squares fit to the data points. The k_{cat} of the reaction was 0.1 s^{-1}.

formation by R118A using QA was measured by the manually quenched radiolabel transfer method. The initial rate of NAMN formation was linear, at 2×10^{-5} s^{-1}, consistent with the steady-state k_{cat} value (2.4×10^{-4} s^{-1}). For R152A using QA, the initial rate of NAMN formation was also linear at 0.1 s^{-1}, consistent with its steady-state k_{cat} value (Figure 5).

For the K185A mutant, chemical quench experiments performed with [^{3}H]QA as the substrate revealed a pre-steady-state burst of [^{3}H]NAMN formation, followed by a slow linear rate (Figure 6). The scatter in the data is due to the low activity of the mutant enzyme. Nevertheless, the existence of a pre-steady-state burst was reproducible, with an amplitude of 0.9 ± 0.1 mol of [^{3}H]NAMN/mol of K185A. A relatively fast pre-steady-state rate of 0.01 s^{-1} and a slower steady-state rate of 0.00013 s^{-1} (0.008 min^{-1}) provided a good fit to the data. In contrast to WT, the presence of a burst of [^{3}H]NAMN formation by K185A when utilizing [^{3}H]QA indicates a relatively fast chemistry step for the mutant enzyme, with either product release or further processing providing the rate limitation.

To confirm this implication, rapid quench experiments were performed with K185A using [^{14}C]NA as the substrate. In direct

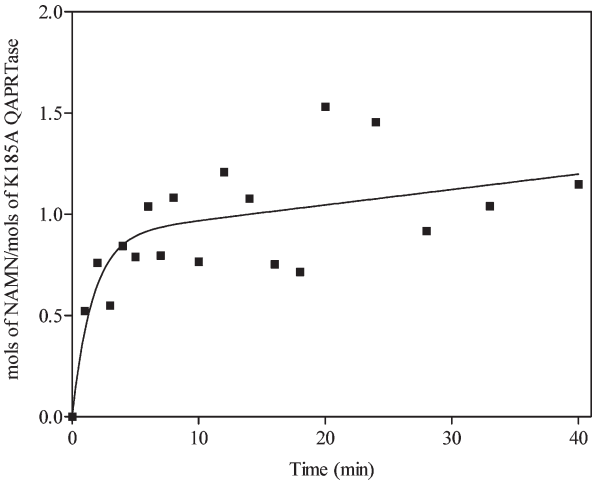

FIGURE 6: [^{3}H]NAMN formation by K185A with [^{3}H]QA in the pre steady state. Rapid mixing was performed manually as described in Materials and Methods. The curve represents the best fit of the data to eq 1, with rate constants equal to 0.01 s^{-1} and 0.00013 s^{-1} for the pre steady state and steady state, respectively.

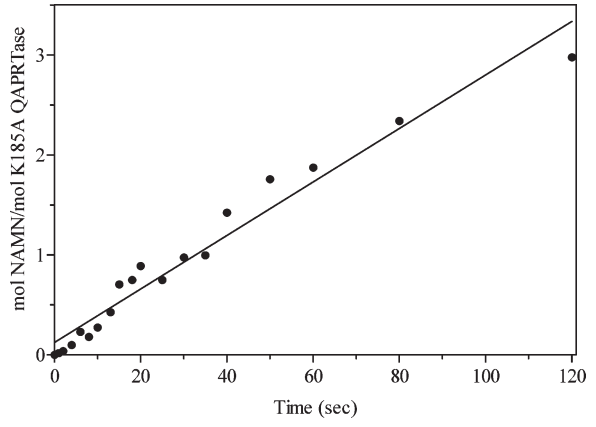

FIGURE 7: Pre-steady-state kinetics of [^{14}C]NAMN formation by K185A with [^{14}C]NA. Rapid mixing was performed in the Kintek chemical-quench-flow apparatus as described in Materials and Methods. The solid line represents a linear least-squares fit to the data points. The k_{cat} of the reaction was 0.03 s^{-1}.

contrast to the reaction of K185A with [^{3}H]QA, the pre-steady-state result of K185A with [^{14}C]NA showed no burst of NAMN formation (Figure 7). The initial rate was linear at 0.03 s^{-1}, in agreement with the steady-state k_{cat} value for NA (0.05 s^{-1}) and, in particular, in rough agreement with the pre-steady-state burst rate (0.01 s^{-1}) of product formation for the reaction of K185A with QA. The result of the reaction of K185A with NA suggests that the release of NAMN as observed for WT is not rate-limiting in the use of QA by this mutant. Therefore, it must be that for the reaction of K185A with QA an intermediate was formed, whose subsequent reaction or release was rate-limiting.

The burst of on-enzyme product formation by K185A with [^{3}H]QA suggests the existence of an intermediate whose further reaction may limit the turnover. On paper chromatography, the behavior of the products from the reaction of K185A with [^{3}H]QA was similar to that of NAMN.

Restoration of Enzymatic Activity by Mutant Complementation. In the *S. typhimurium* QAPRTase dimer, Arg118′ interacts with QA across the subunit interface. R118A was used as a probe in complementation experiments with other debilitated or inactive mutant enzymes to test the importance of this

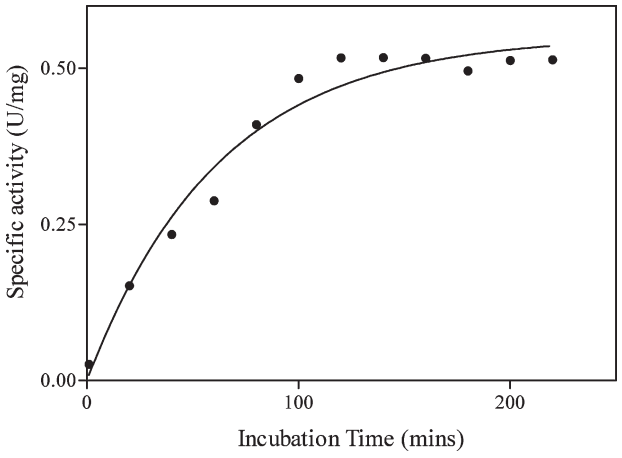

FIGURE 8: Time-dependent complementation of the inactive R175A mutant. Poorly active R118A mutant was mixed with equimolar R175A as described in Materials and Methods. The line represents a fit of the data to a single exponential function.

Table 3: Activity of Complementation Mixtures Containing R118A[a]

complementing enzyme	specific activity (units mg^{-1})	mixture (1:1) tested	specific activity (units mg^{-1})
WT	1	R118A/WT	1.1
R152A	0.03	R118A/R152A	0.5
K153A	ND[b]	R118A/K153A	0.4
R175A	ND	R118A/R175A	0.5
K185A	1.6×10^{-3}	R118A/K185A	0.5

[a]Activity of R118A was 2.4×10^{-4} units mg^{-1}. [b]ND, not detected.

interfacial participation. Incubation of equal molar concentrations of R118A with R175A resulted in restoration of enzymatic activity (Figure 8). Similar results were observed with R152A and K185A. The restoration of activity was maximal within about 2−3 h. The activities of individual mutants and the activities of equimolar mixtures of R118A with mutant enzymes are presented in Table 3, as percentages of the activity of WT enzyme. The general observation is that mixing R118A with all poorly active or with inactive mutants restored activity. The R118A mutant enzyme also complemented other poorly active mutants (E214A, E214D, K153A, and K284) described in the preceding paper. However, mixing binary combinations from among R152A, K153A, R175A, E214A, E214D, and K284A did not restore enzyme activity (unpublished results). Because the enhanced activity was observed only in the presence of R118A, it is most likely associated with formation of heterodimers between the two mutants. Because the activities of the equilibrated heterodimeric mutants were about 50% of WT, the most logical explanation is that one of the two active sites of the dimer can function at full activity with the other in an inactive state and that heterodimers are preferred in mixtures of R118A with the other mutants.

DISCUSSION

The site-directed mutagenic investigation of the conserved residues at the QA binding site of QAPRTase showed that the interactions made by the residues are important for binding and catalysis. Lys185 most likely plays a direct chemical role in the stability of the QAMN ylide intermediate in the decarboxylation

step, and it is a substrate specificity determinant for QAPRTase. Arg152 functions in QA binding and substrate discrimination. The very low activities of the enzyme mutated at Arg175 implied that the residue is essential and might play a role in both QA and PRPP binding. The importance of head to tail domain swapping (*3*) in QAPRTase is highlighted by Arg118′ as one of the critical participants across the dimer interface.

The hydrogen bond provided to the 2-carboxylate of QA by Lys185 appears by design to bind QA and confer base specificity for QAPRTase. The Lys185 side chain is one that makes a notable conformational change between different complexes. In the *Mycobacterium* apoenzyme structure, the side chain amino group lies close to the carboxylates of Asp186 and Asn187. In the *Salmonella* QA binary complex, the side chain has repositioned and compacted to bind to the QA 2-carboxylate. In neither state does the side chain position appear to preclude base NA binding. The interaction at C2 could potentially stabilize the negative charge at the 2 position on the putative QAMN ylide intermediate that results from decarboxylation. The major catalytic role of Lys185 is demonstrated by the significant decrease in catalysis by K185A. Ablation of the Lys185 side chain to eliminate its interactions with the 2-carboxylate of QA resulted in a weakened binding affinity for QA, an inability to discriminate against NA, and therefore a lack of QA specificity. The base specificity of K185A is the reverse of WT, with WT favoring QA over NA by 2000-fold and K185A exhibiting a 300-fold increase in catalytic efficiency for NA over QA. The reverse base discrimination by K185A enzyme clearly supports a major role for Arg152 in QA binding and specificity. The role of Lys185 in substrate determination reconciles with the change in conformation of Lys185, as observed in the crystal structure of the *Mycobacterium* enzyme upon binding of QA (*6*).

The weak binding affinities of R152A and K185A enzymes for QA suggest roles for these residues in binding QA. The role of Arg152 and Lys185 in catalytic substrate discrimination was addressed from the ability of R152A and K185A to utilize NA as a substrate.

The pre-steady-state burst observed for K185A when QA is utilized as the substrate indicated that formation of an initial product was fast, and either its release or further modification was slow. However, the rapid linear reaction of K185A using NA as the substrate indicated a difference in product formation. If the initial burst product of K185A reaction with QA were NAMN, its further kinetic behavior would be similar to the product of the K185A reaction with NA, which is without question NAMN. The presence of a slower steady-state rate for the reaction of K185A with QA implied that the product that formed was not NAMN. An explanation of the burst of product formation for the reaction of K185A with QA is that the putative QAMN intermediate was formed, and either the decarboxylation of QAMN or its release into solution is the rate-limiting step. Attempts to detect the QAMN intermediate were unsuccessful. The unstable nature of the putative QAMN intermediate might not have permitted its capture under the current isolation procedure. The pre-steady-state experiment with K185A strongly suggests that Lys185 participates in the decarboxylation step of QAPRTase and most likely uses its positive charge to stabilize the negative charge of the QAMN ylide intermediate. Lysine residues are known to be carbamoylated by carbon dioxide, usually to form a catalytically stable part of a metal ion binding site. We note with interest the possibility that a lysine residue acts catalytically and covalently accepts the initial carbon dioxide of *Vibrio cholerae* oxaloacetate decarboxylase (*19*). A water molecule found associated with the amino of Lys185 noted in some complexes of the yeast QAPRTase (*22*) could potentially represent a carboxylysine.

The importance of Arg118′ in catalysis is supported by several results. First, the location of Arg118 within the active site, forming hydrogen bonds to both substrates but stretching across the subunit in crystal structures, suggested a catalytic role. Second, sequence analysis showed absolute conservation of Arg118′. Third, mutation to alanine resulted in a dramatic decrease in the catalytic efficiency for PRPP due to the reduced k_{cat} and a higher K_m value for PRPP. Finally, the undetectable binding of PRPP to R118A strongly indicates an important role for Arg118′ in PRPP binding.

The observed restoration of the activity of inactive and poorly active mutants when mixed with R118A supports the structural studies in the interfacial participation of Arg118′ in catalysis. Dimerization facilitates proper structural alignment of the otherwise distant and essential Arg118′ residue from the adjacent subunit in the active site of QAPRTase. Earlier work by Ozturk et al. (*27*) has also shown that a type I PRTase, OPRTase, possesses this property of active site sharing of residues from the adjacent subunit. OPRTase has a flexible loop containing the Lys103 residue that is required for activity. Like QAPRTase in capping the enzyme active site, the loop in OPRTase acts as a lid for the active site formed by the adjacent subunit of the homodimer. In the OPRTase relative HGPRTase, the homologous loop is provided by the same subunit (*28*).

The very weak binding of R152A and K185A mutant enzymes to PRPP was unexpected, for neither of the residues interacts directly with PRPP. The likeliest explanation for this observation is that the web of hydrogen bonds formed by residues interacting with QA (Figure 2) was disrupted, possibly via Arg118. Additionally, other residue−residue interactions appear important. In the *M. tuberculosis* QAPRTase·PA·PRPPC ternary complex, Arg152, which does not interact with PRPP, is sequence adjacent to Lys153, which does. Arg152 is also seen to interact with the main chain of Asn122′, which, in turn, forms a hydrogen bond with main chain of Arg118′. Lys185, which does not interact with PRPP, is adjacent to Asp173, which does.

REFERENCES

1. Musick, W. D. (1981) Structural features of the phosphoribosyltransferases and their relationship to the human deficiency disorders of purine and pyrimidine metabolism. *CRC Crit. Rev. Biochem. 11*, 1–34.
2. Eads, J. C., Ozturk, D., Wexler, T. B., Grubmeyer, C., and Sacchettini, J. C. (1997) A new function for a common fold: the crystal structure of quinolinic acid phosphoribosyltransferase. *Structure 5*, 47–58.
3. Chappie, J. S., Canaves, J. M., Han, G. W., Rife, C. L., Xu, Q., and Stevens, R. C. (2005) The structure of a eukaryotic nicotinic acid phosphoribosyltransferase reveals structural heterogeneity among type II PRTases. *Structure 13*, 1385–1396.
4. Shin, D. H., Oganesyan, N., Jancarik, J., Yokota, H., Kim, R., and Kim, S. H. (2005) Crystal structure of a nicotinate phosphoribosyltransferase from *Thermoplasma acidophilum*. *J. Biol. Chem. 280*, 18326–18335.
5. Wang, T., Zhang, X., Bheda, P., Revollo, J. R., Imai, S., and Wolberger, C. (2006) Structure of Nampt/PBEF/visfatin, a mammalian NAD^+ biosynthetic enzyme. *Nat. Struct. Mol. Biol. 13*, 661–662.
6. Sharma, V., Grubmeyer, C., and Sacchettini, J. C. (1998) Crystal structure of quinolinic acid phosphoribosyltransferase from *Mycobacterium tuberculosis*: a potential TB drug target. *Structure 6*, 1587–1599.

7. Foster, J. W., and Moat, A. G. (1978) Mapping and characterization of the *nad* genes in *Salmonella typhimurium* LT-2. *J. Bacteriol. 133*, 775–779.
8. Holley, E. A., and Foster, J. W. (1982) Bacteriophage P22 as a vector for Mu mutagenesis in *Salmonella typhimurium*: isolation of *nad-lac* and *pnc-lac* gene fusions. *J. Bacteriol. 152*, 959–962.
9. Foster, J. W., Kinney, D. M., and Moat, A. G. (1979) Pyridine nucleotide cycle of *Salmonella typhimurium*: isolation and characterization of *pncA*, *pncB*, and *pncC* mutants and utilization of exogenous nicotinamide adenine dinucleotide. *J. Bacteriol. 137*, 1165–1175.
10. Foster, J. W., and Moat, A. G. (1980) Nicotinamide adenine dinucleotide biosynthesis and pyridine nucleotide cycle metabolism in microbial systems. *Microbiol. Rev. 44*, 83–105.
11. Mann, D. F., and Byerrum, R. U. (1974) Quinolinic acid phosphoribosyltransferase from castor bean endosperm. I. Purification and characterization. *J. Biol. Chem. 249*, 6817–6823.
12. Kalikin, L., and Calvo, K. C. (1988) Inhibition of quinolinate phosphoribosyl transferase by pyridine analogs of quinolinic acid. *Biochem. Biophys. Res. Commun. 152*, 559–564.
13. Cao, H., Pietrak, B. L., and Grubmeyer, C. (2002) Quinolinate phosphoribosyltransferase: kinetic mechanism for a type II PRTase. *Biochemistry 41*, 3520–3528.
14. Bhatia, R., and Calvo, K. C. (1996) The sequencing expression, purification, and steady-state kinetic analysis of quinolinate phosphoribosyl transferase from *Escherichia coli*. *Arch. Biochem. Biophys. 325*, 270–278.
15. Rozenberg, A, and Lee, J. K. (2008) Theoretical studies of the quinolinic acid to nicotinic acid mononucleotide transformation. *J. Org. Chem. 73*, 9314–9319.
16. Brown, E. V., and Moser, R. J. (1971) Further evidence as to the nature of the transition state leading to decarboxylation of 2-pyridinecarboxylic acids. Electrical effects in the transition state. *J. Org. Chem. 36*, 454–457.
17. Dunn, G. E., and Thimm, H. F. (1977) Kinetics and mechanism of decarboxylation of some pyridine carboxylic acids in aqueous solution. *Can. J. Chem. 55*, 1342–1347.
18. Harris, P., Navarro Poulsen, J. C., Jensen, K. F., and Larsen, S. (2000) Structural basis for the catalytic mechanism of a proficient enzyme: orotidine 5′-monophosphate decarboxylase. *Biochemistry 39*, 4217–4224.
19. Studer, R., Dahinden, P., Wang, W. W., Auchli, Y., Li, X.-D., and Dimroth, P. (2007) Crystal structure of the carboxyltransferase domain of the oxaloacetate decarboxylase Na^+ pump from *Vibrio cholerae*. *J. Mol. Biol. 367*, 547–557.
20. Kim, M. K., Im, Y. J., Lee, J. H., and Eom, S. H. (2006) Crystal structure of quinolinic acid phosphoribosyltransferase from *Helicobacter pylori*. *Proteins 63*, 252–255.
21. Liu, H., Woznica, K., Catton, G., Crawford, A., Botting, N., and Naismith, J. H. (2007) Structural and kinetic characterization of quinolinate phosphoribosyltransferase (hQPRTase) from *Homo sapiens*. *J. Mol. Biol. 373*, 755–763.
22. di Luccio, E., and Wilson, D. K. (2008) Comprehensive X-ray structural studies of the quinolinate phosphoribosyl transferase (BNA6) from *Saccharomyces cerevisiae*. *Biochemistry 47*, 4039–4050.
23. Guex, N., and Peitsch, M. C. (1997) SWISS-MODEL and the Swiss-Pdb Viewer: an environment for comparative protein modeling. *Electrophoresis 18*, 2714–2723.
24. Bello, Z. I., Stitt, B. L., and Grubmeyer, C. (2010) Interactions at the 2 and 5 positions of 5-phosphoribosyl pyrophosphate are essential in *Salmonella typhimurium* quinolinate phosphoribosyltransferase, Biochemistry (DOI 10.1021/bi9018219).
25. Johnson, K. A. (1992) Transient-state kinetic analysis of enzyme reaction pathways, in The Enzymes, pp 1−61, Academic Press, New York.
26. Hughes, K. T., Dessen, A., Gray, J. P., and Grubmeyer, C. (1993) The *Salmonella typhimurium* nadC gene: sequence determination by use of Mud-P22 and purification of quinolinate phosphoribosyltransferase. *J. Bacteriol. 175*, 479–486.
27. Ozturk, D. H., Dorfman, R. H., Scapin, G., Sacchettini, J. C., and Grubmeyer, C. (1995) Locations and functional roles of conserved lysine residues in *Salmonella typhimurium* orotate phosphoribosyltransferase. *Biochemistry 34*, 10755–10763.
28. Eads, J. C., Scapin, G., Xu, Y., Grubmeyer, C., and Sacchettini, J. C. (1994) The crystal structure of human hypoxanthine-guanine phosphoribosyltransferase with bound GMP. *Cell 78*, 325–334.